The Journal of Clinical Endocrinology & Metabolism, 2024, **109**, 2433–2443
https://doi.org/10.1210/clinem/dgae411
Advance access publication 18 June 2024
Clinical Research Article

Double CYP11B1/CYP11B2 Immunohistochemistry and Detection of KCNJ5 Mutations in Primary Aldosteronism

Brasilina Caroccia,[1,2,*] Livia Lenzini,[1,*] Giulio Ceolotto,[1] Francesca Gioco,[1] Andrea Benetti,[3] Alessandra Giannella,[3] Hala Ajjour,[1] Francesca Galuppini,[4] Gianmaria Pennelli,[4] Teresa Maria Seccia,[1] Celso Gomez-Sanchez,[5] and Gian Paolo Rossi[1]

[1]Specialized Center of Excellence for Hypertension of the European Society of Hypertension and Emergency Medicine Unit, Department of Medicine-DIMED, University of Padua, Padua 35126, Italy
[2]Department of Women's and Children's Health-SBD, University of Padua, Padua 35122, Italy
[3]Division of Thrombotic and Hemorrhagic Diseases, Department of Medicine-DIMED, University of Padua, Padua 35122, Italy
[4]Department of Medicine, Surgical Pathology Unit, University of Padua, Padua 35122, Italy
[5]G.V. (Sonny) Montgomery VA Medical Center and Department of Pharmacology and Toxicology, University of Mississippi Medical Center, Jackson, MS 39216, USA

Correspondence: Prof. Gian Paolo Rossi, MD, DIMED– Hypertension Unit, University Hospital, Via Giustiniani, 2, 35126 Padova, Italy. Email: gianpaolo.rossi@unipd.it.
*These Authors equally contributed to the work.

Abstract

Context: The search for somatic mutations in adrenals resected from patients with primary aldosteronism (PA) is performed by Sanger sequencing, often implemented with immunohistochemistry (IHC)-guidance focused on aldosterone-producing (CYP11B2-positive) areas.

Objective: To investigate the impact of double IHC for CYP11B1 and CYP11B2 on Sanger and next-generation sequencing (NGS).

Methods: We investigated 127 consecutive adrenal aldosterone-producing adenomas from consenting surgically cured PA patients using double IHC for CYP11B1 and CYP11B2, by Sanger sequencing and NGS.

Results: Double IHC for CYP11B2 and CYP11B1 revealed 3 distinct patterns: CYP11B2-positive adenoma (pattern 1), mixed CYP11B1/CYP11B2-positive adenoma (pattern 2), and adrenals with multiple small CYP11B2-positive nodules (pattern 3). Sanger sequencing allowed detection of KCNJ5 mutations in 44% of the adrenals; NGS revealed such mutations in 10% of those negative at Sanger and additional mutations in 61% of the cases. Importantly the rate of KCNJ5 mutations differed across patterns: 17.8% in pattern 1, 71.4% in pattern 2, and 10.7% in pattern 3 ($\chi^2 = 22.492$, $P < .001$).

Conclusion: NGS allowed detection of mutations in many adrenals that tested negative at Sanger sequencing. Moreover, the different distribution of KCNJ5 mutations across IHC patterns indicates that IHC-guided sequencing protocols selecting CYP11B2-positive areas could furnish results that might not be representative of the entire mutational status of the excised adrenal, which is important at a time when KCNJ5 mutations are suggested to drive management of patients with aldosterone-producing adenomas.

Key Words: primary aldosteronism, next-generation sequencing, kir3.4 channel, CYP11B2 immunohistochemistry, Sanger sequencing

Abbreviations: APA, aldosterone-producing adenoma; IHC, immunohistochemistry; NGS, next-generation sequencing; PA, primary aldosteronism; PCR, polymerase chain reaction; uPA, unilateral primary aldosteronism; VAF, variant allele frequency.

The discovery of gene mutations in patients with primary aldosteronism (PA) has opened a curtain on the molecular mechanisms that underpin this common curable cause of human arterial hypertension, both in sporadic cases and, less commonly, in familial forms (1, 2). Using Sanger sequencing, a large international multicenter study identified mutations involving the Kir3.4 channel (*KCNJ5*) in 34% of the aldosterone-producing adenoma (APA) patients (3). A meta-analysis of a large multiethnic cohort of APA patients thereafter evidenced prominent differences of KCNJ5 mutations prevalence across continents and ethnicities (4). It was then contended that these diversities could reflect the differences across countries/continents in broadness of screening strategies, age at diagnosis, and population salt consumption (4). However, the sensitivity of the methodologies exploited for searching the mutations could be a further reason underlying these disparities. Currently, 2 main methods are used to this end: Sanger sequencing and next-generation sequencing (NGS) (5) which has been recently improved to achieve a high resolution (6).

In 2014, the development, in Gomez-Sanchez's laboratory, of specific monoclonal antibodies for human aldosterone synthase (cytochrome P450, family 11, subfamily B, polypeptide 2 [CYP11B2]) and 11β-hydroxylase (cytochrome P450, family 11, subfamily B, polypeptide 2 [CYP11B1]) opened to road to immunochemical detection of aldosterone-producing and cortisol-producing cells in the resected adrenals (7, 8) and,

Received: 15 March 2024. **Editorial Decision:** 9 June 2024. **Corrected and Typeset:** 4 July 2024

therefore, to immunohistochemistry (IHC)-guided sequencing. By allowing the physical selection of aldosterone-producing cells putatively carrying the mutations through the scraping of the region positive to CYP11B2, IHC was hypothesized to increase the detection rate of mutations (9, 10). However, IHC-guided sequencing for either Sanger or NGS is time-consuming and unsuitable for routine use outside of a few research centers, which represents a major hurdle to its routine use. Thus, even though IHC-guided sequencing strategies could increase the detection rate of mutations in PA hot spot genes (9, 10), like *KCNJ5* (1) and others, such as ATPase Na^+ /K^+ transporting, 1-polypeptide (*ATP1A1*) (11, 12), ATPase Ca^{2+}-transporting, plasma membrane 3 (*ATP2B3*) (12), Calcium channel, voltage-dependent, L-type, 1D-subunit (*CACNA1D*) (11, 13) and Calcium channel, voltage-dependent, T-type, 1H-subunit (*CACNA1H*) (14), easier and faster methods for searching the mutations are highly desirable at a stage when a precision medicine strategy for the treatment of PA patients with KCNJ5 mutations is being pursued (15-17). The role of these mutations in increasing aldosterone secretion has been reviewed in depth elsewhere (2).

However, a thorough search of the literature using the keywords "*aldosterone producing adenoma*," "*KCNJ5*," "*Sanger sequencing*," and "*next generation sequencing*" and the Boolean operators "AND" and "OR" revealed no systematic comparison of accuracy between Sanger sequencing with NGS for the detection of KCNJ5 mutations. Moreover, there is no information regarding the yield of these techniques in adrenal specimen submitted to double IHC for CYP11B1 and CYP11B2.

Thus, taking advantage of our systematic application of double IHC using highly specific monoclonal antibodies for human CYP11B1 and CYP11B2 (18) to resected adrenals and of a series of PA patients who were unambiguously biochemically cured after unilateral adrenalectomy, we set out this study to investigate if: (i) the rate of identified KCNJ5 mutations was affected by the double IHC pattern; and (ii) NGS could increase the rate of identification of KCNJ5 somatic mutations over Sanger sequencing in resected adrenals of patients with PA. The novel knowledge generated in this field can substantively increase the detection of KCNJ5 mutations in PA with relevant implications for clinical management of these patients as cells carrying these common mutations can be exquisitely sensitive to macrolides (15-17).

Methods

Patients

We recruited for this study 127 consecutive patients with unilateral PA (uPA), who signed the informed consent and were submitted to adrenal vein sampling–guided laparoscopic adrenalectomy. All were unequivocally diagnosed with PA according to current specific guidelines (19-21). Serum K^+ levels, plasma aldosterone concentration, plasma active renin concentration and the aldosterone-renin ratio were measured as reported (22).

Tumor specimens were collected in the operating room, immediately after surgery, with utmost precaution to ensure the preservation of nucleic acids, tissue structure, and morphology. A trained pathologist (F.G.) identified the adenoma or the nodule(s) and the adjacent tissue in the operating room. Multiple parts of the APA or nodule(s) were collected, immediately snap-frozen into isopentane vial precooled on dry ice, and stored in liquid nitrogen until sequencing was performed as described below. Pathology and immunohistochemistry of adjacent paraformaldehyde-fixed tumor sections were prepared in all resected adrenals. For double IHC, they were exposed to monoclonal antibodies for human aldosterone synthase (CYP11B2) and 11β hydroxylase (CYP11B1) (23). None of the PA patients showed concurrent cortisol production and all patients showed biochemical cure according to the PASO criteria (24).

All patients consented to use their resected adrenal gland for research purposes. The samples were systematically collected in the institutional biobank, which was approved by the institutional ethics committee (Comitato Etico Territoriale Area Centro-Est Veneto, Padova, Italy, Approval number: 1925P).

Double CYP11B1/CYP11B2 Immunohistochemistry and Immunofluorescence

Double CYP11B1/CYP11B2 IHC was performed in all 127 tissues. The details for performing double CYP11B1 (RRID: AB_2650563)/CYP11B2 (RRID: AB_2650562) IHC and immunofluorescence were previously reported (23).

Sanger Sequencing

After DNA extraction using the QIAamp DNA Mini Kit (Qiagen, Milan, Italy), adrenal specimens (n = 127) were sequenced using Sanger sequencing of *KCNJ5* with standard methods following polymerase chain reaction (PCR) amplification, as reported (23). PCR was performed to amplify genomic fragments of the KCNJ5 gene using Sso Fast EVA Green Supermixes (Bio-Rad, Los Angeles, CA, USA) and specific primers (forward, 5′-CGACCAAGAGTGGATTCCTT-3′, and reverse, 5′-AGGGTCTCCGCTCTCTTCTT-3′). Purification of PCR products was done using the PCR Purification Kit (Qiagen, Milan, Italy).

Direct sequencing of PCR products spanning amino acids 122 to 199 was performed using the ABI Prism Big Dye Terminator version 3.1 cycle sequencing kit (Applied Biosystems, Foster City, CA, USA) on an ABI Prism 3700 DNA analyzer (Applied Biosystems, Milan, Italy).

Next-Generation Sequencing

All samples negative for the KCNJ5 somatic mutations (n = 71) at Sanger sequencing and 41 patients carrying the mutations were sequenced by targeted capture NGS, using a custom panel of biotinylated oligonucleotides (xGen™ Hyb Panel, Integrated DNA Technologies, Coralville, Iowa, USA). The latter consists of 487 amplicons covering coding regions and flanking exon/intron boundaries of 12 PA putative genes (*KCNJ5, ATP1A1, ATP2B3, CTNNB1, CACNA1D, APC, CACNA1H, PRKACA, ARMC5, GNA11, GNAQ, CLCN2*), which provided an average gene coverage > 99% at 500X. The libraries for targeted capture were prepared using the Lotus DNA library prep Kit (IDT). Briefly, 100 ng of DNA was quantified by Qubit DNA HS assay (Life Technologies, Milan, Italy). Genomic DNA was enzymatically cut; fragments were then ligated with stubby P5 and P7 adapters, following the manufacturer's instructions.

AMPure XP beads (Beckman Coulter, Brea, CA, USA) were used to purify the libraries, which were quantified by LabChip GX Touch Nucleic Acid Analyzer (PerkinElmer, Boston, MA, USA). A multiplexing pool of 500 ng of each library from 12

samples was used for hybrid capture with the biotinylated DNA oligonucleotides custom panel. After hybridization, Streptavidin Dynabeads were used to capture biotinylated DNA. Purified DNA was amplified using the Bio-Rad CX200 thermal cycler (Bio-Rad Laboratories, Hercules, USA). The library pool was further purified using AMPure XP beads (Beckman Coulter, Brea, USA) and quantified by Qubit DNA HS assay. Amplicon length average size was 254. Finally, libraries were sequenced on an Illumina MiSeq at a final concentration of 12 pM using a v3 cartridge (2 × 151 reads) following the manufacturer's instructions. This high-resolution NGS method was found to provide a high Qscore of 30 (Q30) of 99.9%, indicating that the base call accuracy (ie, the probability of a correct base call) is higher compared with other available methods (6, 25).

Bioinformatic Analysis

A file detailing the sequence of the hybridizing oligonucleotides, and the coordinates of designed amplicons, downloaded from the manufacturer (IDT, Tema Ricerca, Milan, Italy) was uploaded into the CLC genomics Workbench (vers. 23.0.5) and in the Enrichment app (vers. 3.1) (Base Space, Illumina, Milan, Italy). The sequencing reads were aligned to the human reference sequence HG19, and the workflow then removed ligation artifacts from the read mapping. Next, the Indels and Structural Variants detection step generated a guidance track used for improving the mapping with the Local Realignment tool. Variant allele frequency (VAF) was then detected using the Low Frequency Variant Detection tool for somatic variant detection (frequency of < 2%), and the Fixed Ploidy Variant Detection tool for germline applications (> 30%). Finally, a series of filtering steps was applied to remove variants that likely entailed artifacts. Low VAF is often confounded by sequencing errors that generally occur at a rate of ~1% per base on Illumina platforms, as well as DNA polymerase errors during PCR enrichment. To fix these errors, we added unique molecular index (UMIs), as barcodes, to the sequencing reads, because this has been shown to substantially improve the accuracy of detecting lower VAFs by reconstructing consensus sequences with error correction (6). The final output of the workflow produces a list of filtered variants, including some present at very low frequency and BAM files which are visualized in IGV (Integrative Genomics Viewer). The concordance of the 2 different pipelines was found to be 100% in our hands.

Statistical Analysis

Data were analyzed with SPSS (vers. 29, IBM, Bologna Italy) and Prism (GraphPad Prism version 10.1.1 for MAC, GraphPad Software, Boston, Massachusetts USA, www.graphpad.com). They are presented as rate and mean + SD, or median and interquartile range (IQR), as appropriate. A first stepwise logistic regression (Wald backward with PIN = 0.10 and POUT = 0.15) was performed to identify the predictors of Sanger-negative sequencing results in the entire population and to determine the correct classification rate (26).

To assess the impact of the VAF, which is furnished only by NGS, on Sanger-negative results, a second similar analysis was performed in the sub-cohort of 48 resected adrenals with a mutation in KCNJ5 found with Sanger sequencing which were also analyzed by NGS, by entering VAF among the potential predictors.

Table 1. Main clinical features of the 127 patients before and 1 month after adrenalectomy

	Baseline	Postadrenalectomy	*P*
Age, years	52 ± 10	—	
Ethnicity	Caucasian		
BMI, kg/m^2	26 ± 3.8	—	
Sex M/F, n (%)	74 (58)	—	
SBP, mmHg	157 ± 19	130 ± 13	<.001
DBP, mmHg	93 ± 14	80 ± 9	<.001
Serum K$^+$, mmol/L	3.5 ± 0.5	4.3 ± 0.5	<.001
PAC, ng/dL	20.4 (17.5-24.2)	6.1 (5.0-8.4)	<.001
DRC, mIU/L	2.2 (2.0-4.1)	7.2 (3.3-12.0)	<.001
ARR, ng/mIU	63.8 (32.4-129.7)	11.3 (6.3-27.4)	<.001

Data are presented as mean ± SD or median (IQR), as appropriate.
Abbreviations: ARR, aldosterone to renin ratio; BMI, body mass index; DBP, diastolic blood pressure; DRC, direct renin concentration; K$^+$, potassium; PAC, plasma aldosterone concentration; SBP, systolic blood pressure.

Results

Patients

Table 1 shows the main clinical features of the 127 consenting adrenalectomized PA patients recruited for this study who underwent Sanger sequencing and NGS and IHC classification, as shown in Fig. 1. Figure 2, which illustrates the changes in plasma aldosterone concentration, plasma active renin concentration, aldosterone-renin ratio, and serum K$^+$ levels, demonstrates unambiguous biochemical cure in all patients after surgery. Of note, plasma active renin concentration remained low in few patients, who needed β-blocker treatment for concomitant cardiovascular conditions.

Identification of KCNJ5 Somatic Mutations by NGS

By applying Sanger sequencing and NGS in 127 consecutive patients with uPA, we found somatic mutations in 84.2%. At Sanger sequencing analysis, 44% of the specimen (n = 56) was positive for the most common KCNJ5 mutations G151R (n = 38), L168R (n = 16), and for 2 rarer mutations, the Glu145_Thr146delinsVal and the insT149 located out of the channel selectivity filter, which was fully functionally characterized (23). Resequencing of the 71 resected adrenals that tested negative at Sanger by NGS unveiled the common *KCNJ5* somatic mutations in 7 additional cases: L168R (n = 5) and G151R (n = 2). These mutations had a variant allele frequency (VAF) varying between 1.0% and 12.9% (Table 2). Thus, in the total cohort, the rate of KCNJ5 mutations increased from 44% with Sanger to 50% with NGS.

NGS also identified mutations in other genes (ATP1A1, CACNA1D, ATP2B3, CTNNB1, CLCN2, CACNA1H, GNAQ, PRKACA, and ARMC5; Table 3); thus, the total frequency of somatic mutations was 84% (107 of 127 patients). Concurrent mutations in 2 genes were found in 10 of the KCNJ5 Sanger-negative patients and an additional mutation was discovered in 3 KCNJ5-positive patients at NGS. Overall, in the 41 resected adrenals with a KCNJ5 mutation at Sanger sequencing, 29% (n = 12) carried an additional mutation when analyzed with NGS (Table 4).

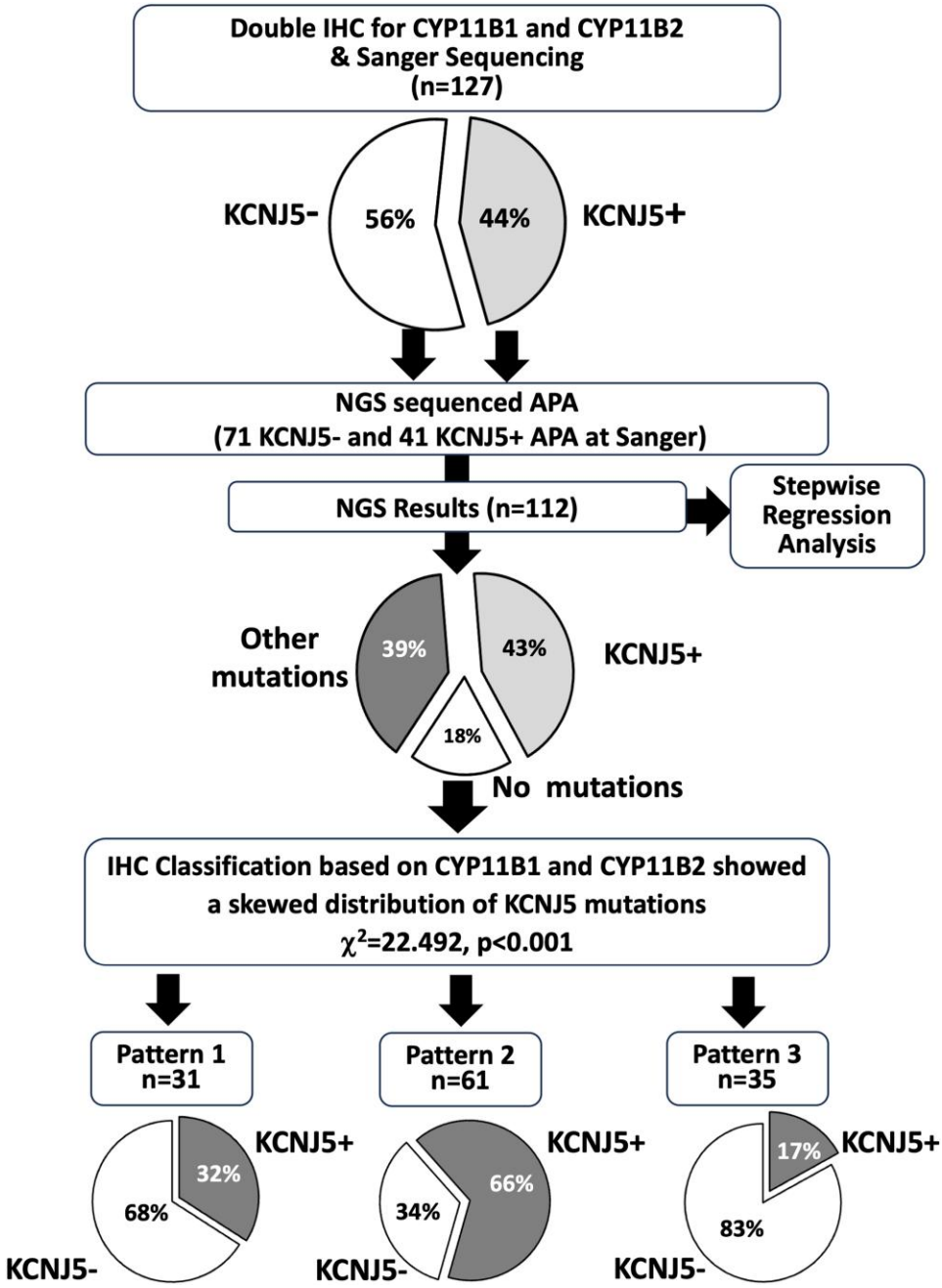

Figure 1. Flow-chart of the study and number of APA patients examined in the different experiments.

Double CYP11B1/CYP11B2 Immunohistochemistry and Immunofluorescence Results

With systematic immune-phenotyping with double CYP11B2 and CYP11B1 IHC of the resected adrenals, we identified 3 different patterns for CYP11B2 and CYP11B1 expression: tumors expressing strongly and almost exclusively CYP11B2 (pattern 1); tumors with expression of both CYP11B2 and CYP11B1 (pattern 2); and specimens with multiple small nodules comprising aldosterone-producing nodule(s) expressing CYP11B2 (pattern 3) (Fig. 3). To investigate whether the expression of CYP11B2 and CYP11B1 coexisted in pattern 2, we also performed immunofluorescence and confocal microscopy imaging. This provided evidence that pattern 2 APA was composed of 3 cell populations, one expressing only CYP11B2, one only CYP11B1, and a much smaller population of cells expressing both steroidogenic enzymes (Fig. 4).

We next examined the distribution of KCNJ5 mutations and other mutations as a function of the 3 patterns identified with IHC. This unveiled a markedly skewed rate of the KCNJ5 mutations: 71.4% of the APA expressing both CYP11B2 and CYP11B1 (pattern 2) had KCNJ5-mutations, while only 17.8% of those expressing only CYP11B2 (pattern 1) had KCNJ5 mutations. The specimens that showed multiple small aldosterone-producing nodules expressing CYP11B2 (pattern 3) had KCNJ5 mutations in 10.7%. Thus, the KCNJ5 mutations were differentially distributed across IHC patterns in a highly significant way ($\chi^2 = 22.5$, $P < .001$, Table 5, Fig. 1).

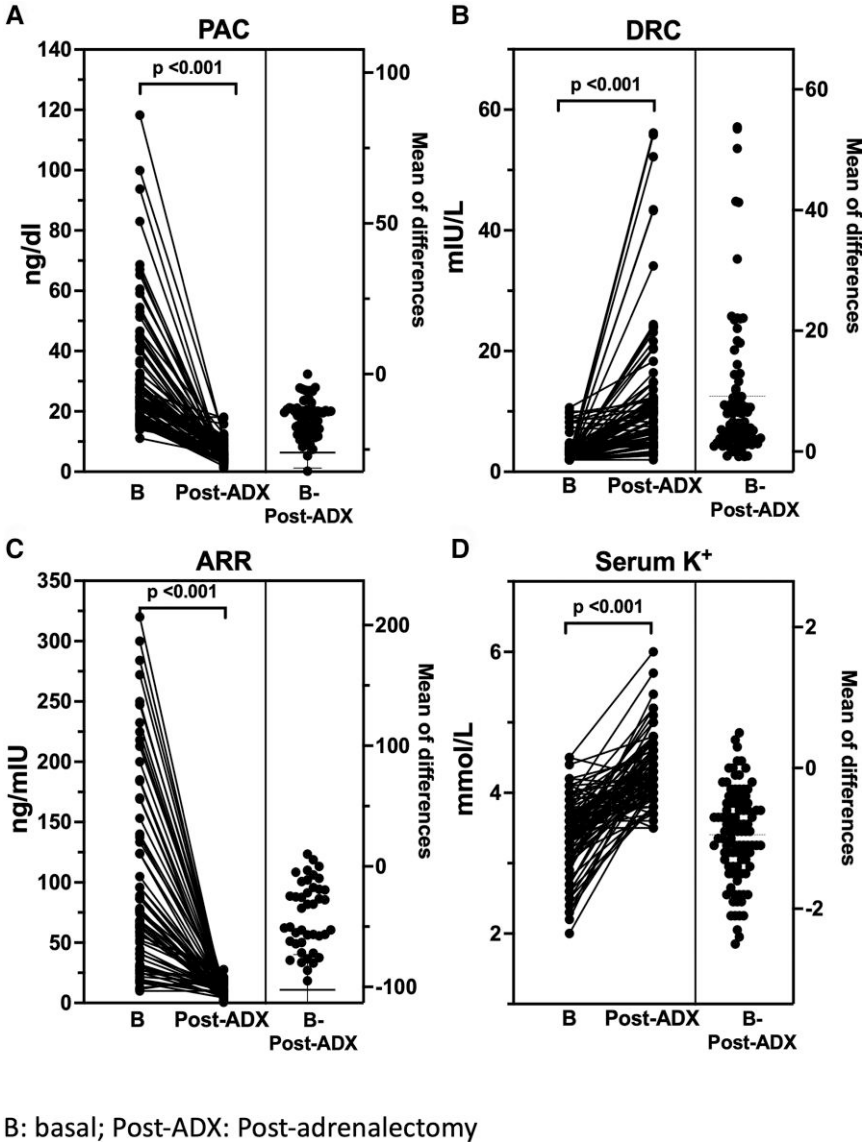

Figure 2. The plots documented the biochemical cure obtained in our 127 uPA patients. The left parts of each plot illustrate the highly significant changes from baseline (B) to post-adrenalectomy (post-ADX) in plasma aldosterone concentration (PAC, panel A), plasma levels of active renin (DRC, panel B) as measured with a chemiluminescent method using a specific antibody recognizing the active site of the enzyme, the aldosterone-renin-ratio (ARR, panel C), and serum K^+ levels (panel D). The estimation plots (right parts of the plots) visually illustrate the size of the change and the significance level.

Table 2. *KCNJ5* mutation identified by NGS in KCNJ5-negative patients at Sanger sequencing

Patient number	Sex	Age	*KCNJ5* somatic mutation	Coding region	VAF (%)	Gene_2	c.DNA	Amino acid change	VAF (%)
2	M	48	L168R	c.503T > G	1.4	*CTNNB1*	c.134C > T	p.Ser45Phe	27.2
29	F	34	L168R	c.503T > G	12.9	—	—	—	—
31	M	49	L168R	c.503T > G	1	*ATP1A1*	c.311T > G	p.Leu104Arg	26.7
48	M	69	L168R	c.503T > G	5.7	—	—	—	—
75	F	57	G151R	c.451G > C	10	—	—	—	—
102	M	36	L168R	c.503T > G	6.5	*CACNA1D*	c.3038G > C	p.Arg1013Thr	31.7
112	M	47	G151R	c.451G > C	12.2	—	—	—	—

Gene_2: Additional mutation found in KCNJ5-positive patient; —: not detected.
Abbreviations: ATP1A1, ATPase Na+ /K+ transporting, 1-polypeptide; CACNA1D, Calcium channel, voltage-dependent, L-type, 1D-subunit; CTNNB1, β-catenin; NGS, next-generation sequencing; VAF, variant allele frequency.

Table 3. Mutational status of KCNJ5 second Sanger-negative APA identified by NGS

Patient number	Gene_1	c.DNA	Amino acid change	VAF (%)	Gene_2	c.DNA	Amino acid change	VAF (%)
3	*ATP2B3*	c.1230_1235delGCTGGT	p.Leu411_Val412del	57.4	—	—	—	—
4	*CLCN2*	dupCGG[a]	p.Arg646_Gln647insArg	44.6	—	—	—	—
8	*CLCN2*	dupCGG[a]	p.Arg646_Gln647insArg	44.7	—	—	—	—
11	*ATP2B3*	c.1230_1235delGCTGGT	p.Leu411_Val412del	43.7	—	—	—	—
12	*GNAq*	c.286A > T	p.Thr96Ser	10.0	—	—	—	—
13	*CACNA1H*	c.2545C > T	p.Pro849Ser	41.6	*ATP2B3*	c.1230_1235delGCTGGT	p.Leu411_Val412del	1.8
14	*ATP1A1*	c.311T > G	p.Leu104Arg	32.4	—	—	—	—
16	*ATP1A1*	c.311T > G	p.Leu104Arg	6.7	—	—	—	—
18	*ATP2B3*	c.1206_1211delGTTCTT	p.Lys402_Phe404delinsAsn	9.6	—	—	—	—
19	*CTNNB1*	c.133T > C	p.Ser45Pro	31.3	*GNAq*	c.142_143delinsTT[b]	p.Gly48Leu	35.2
24	*GNAq*	c.286A > T	p.Thr96Ser	10.2	*ARMC5*	c.968G > C[b]	p.Gly323Ala	48.8
25	*CACNA1D*	c.1207G > C	p.Gly403Arg	22.8	*CACNA1H*	c.4736G > A[b]	p.Arg1579Gln	40.8
28	*ATP2B3*	c.1230_1235delGCTGGT	p.Leu411_Val412del	1.7	—	—	—	—
32	*ATP1A1*	c.311T > G	p.Leu104Arg	27.6	—	—	—	—
33	*ATP1A1*	c.311T > G	p.Leu104Arg	1.7	—	—	—	—
34	*CTNNB1*	c.133T > C	p.Ser45Pro	30.1	—	—	—	—
35	*ATP1A1*	c.311T > G	p.Leu104Arg	2.43	—	—	—	—
36	*CTNNB1*	c.133T > C	p.Ser45Pro	28.4	—	—	—	—
37	*GNAq*	c.286A > T	p.Thr96Ser	5.6	—	—	—	—
38	*CTNNB1*	c.128_137delinsG[b]	p.Ala43_Leu46delinsGly	27.1	—	—	—	—
39	*CACNA1D*	c.2300T > G	p.Phe767Cys	12.1	*CACNA1H*	c.2545C > T	p.Pro849Ser	48.5
40	*CACNA1H*	c.2362C > T[b]	p.Arg788Cys	1.4	—	—	—	—
42	*ATP2B3*	c.1230_1235delGCTGGT	p.Leu411_Val412del	1.45	—	—	—	—
45	*ATP1A1*	c.299_313del	p.Phe100_Leu104del	25.5	*ATP2B3*	c.1230_1235delGCTGGT	p.Leu411_Val412del	1.1
46	*PRKACA*	c.617T > G	p.Leu206Arg	33.1	—	—	—	—
47	*CTNNB1*	c.133T > C	p.Ser45Pro	27.1	—	—	—	—
50	*CTNNB1*	c.134C > T	p.Ser45Phe	16.3	—	—	—	—
55	*CACNA1D*	c.375delG[b]	p.Trp125fs	4.5	—	—	—	—
56	*ARMC5*	c.517C > T[b]	p.Arg173[b]	34.6	—	—	—	—
57	*CACNA1D*	c.2299T > C	p.Phe767Leu	2.6	—	—	—	—
62	*CLCN2*	c.1136T > C[b]	p.Phe379Ser	51	*PRKACA*	c.617T > G	p.Leu206Arg	28.3
63	*CACNA1D*	c.4117G > A[b]	p.Val1373Met	10.5	—	—	—	—
64	*PRKACA*	c.163T > G[b]	p.Phe55Val	1.5	—	—	—	—

(*continued*)

Table 3. Continued

Patient number	Gene_1	c.DNA	Amino acid change	VAF (%)	Gene_2	c.DNA	Amino acid change	VAF (%)
65	*ATP2B3*	c.1230_1235delGCTGGT	p.Leu411_Val412del	32.2	—	—	—	—
73	*CACNA1D*	c.2015C > T	p.Ser672Leu	12.5	—	—	—	—
74	*CACNA1D*	c.1207G > C	p.Gly403Arg	5.9	—	—	—	—
76	*ATP2B3*	c.1230_1235delGCTGGT	p.Leu411_Val412del	1.4	*CACNA1H*	c.2545C > T	p.Pro849Ser	14.9
79	*CTNNB1*	c.134C > T	p.Ser45Phe	31	—	—	—	—
80	*ATP1A1*	c.311T > G	p.Leu104Arg	1.2	—	—	—	—
81	*CACNA1D*	c.1207G > C	p.Gly403Arg	24.5	—	—	—	—
92	*ATP1A1*	c.311T > G	p.Leu104Arg	26.8	*ATP2B3*	c.1230_1235delGCTGGT	p.Leu411_Val412del	2.0
106	*CACNA1D*	c.2299T > G	p.Phe767Val	8.6	—	—	—	—
121	*ATP1A1*	c.311T > G	P.Leu104Arg	26.0	*CACNA1H*	c.1799C > T[a]	p.Ala600Val	48.5
122	*CLCN2*	dupCGG[a]	p.Arg646_Gln647insArg	43.7	—	—	—	—

Abbreviations: *ARMC5*, Armadillo Repeat Containing 5; *ATP1A1*, ATPase Na+ /K+ transporting, 1-polypeptide; *ATP2B3*, ATPase Ca^{2+}-transporting, plasma membrane 3; *CACNA1D*, Calcium channel, voltage-dependent, L-type, 1D-subunit; *CACNA1H*, Calcium channel, voltage-dependent, T-type, 1H-subunit; *CLCN2*, Chloride Voltage-Gated Channel 2; *CTNNB1*, β-catenin; *GNAq*, Guanine Nucleotide Binding Protein (G Protein); *PRKACA*, Protein Kinase CAMP-Activated Catalytic Subunit Alpha; VAF, variant allele frequency; –, not detected.
[a]VUS (variant of uncertain significance) germline mutation checked in tissue and blood.
[b]VUS.

Of note, the other mutations showed an almost even distribution of the IHC patterns: 29.6% in pattern 1, 29.6% in pattern 2, and 40.8% in pattern 3 ($\chi^2 = 1.5$, $P = 0.826$).

Identification of the Determinants of Sanger-Negative KCNJ5 Somatic Mutations

The independent variables, that were entered in a stepwise logistic regression model to identify the predictors of Sanger-negative sequencing results in the entire population, included tumor size, age, systolic and diastolic blood pressure, plasma aldosterone concentration, plasma active renin level, sex, and double IHC pattern (Fig. 5). We used the backward approach (Wald) to minimize the chances of overlooking relevant predictors (27). The only predictors of Sanger-negative results were age (Exp(B) = 1.099, $P < .001$), tumor size (Exp(B) = 1.294, $P = .041$), and systolic blood pressure (Exp(B) = 0.962, $P = .013$), a model entailing these 3 variables furnished an overall rate of correct classification only of 64.6%.

A similar analysis was performed in the sub-cohort that underwent both Sanger and NGS to investigate if the VAF, which is detected only with NGS, could be useful to predict Sanger-negative results (Fig. 5). This analysis showed that, of all predictors, only the VAF remained in the model (Exp(B) = 0.849 (0.762-0.945) $P = .003$) and yielded an overall rate of correct classification of 93.8% (Fig. 5). The original SPSS output of these analyses is given in the online repository (27).

Discussion

KCNJ5 mutations are the most prevalent in all ethnicities of unilateral PA patients except among Black individuals (28). Seminal discoveries suggested that detection of these mutations can lead to specific pharmacological treatment with macrolide antibiotics and their derivatives (15-17) and therefore to a precision medicine treatment of PA. We, therefore, compared the rate of *KCNJ5* mutations detected with Sanger and NGS sequencing in patients with unilateral PA (uPA), as confirmed by biochemical cure after surgery (Fig. 2). The systematic assessment of the adrenals excised from these patients with double IHC using specific monoclonal antibody for CYP11B2 and CYP11B1 (Fig. 3) allowed us to examine the distribution of KCNJ5 mutations according to the 3 more common immunochemical patterns, which unveiled a key novel piece of knowledge with relevant implications for genotyping, as discussed below.

The first important finding of this study was that targeted NGS allowed the detection of KCNJ5 mutations in a larger proportion of the specimens judged to be wild-type by Sanger sequencing, even when the VAF was as low as 1%. At a logistic stepwise regression analysis, the Sanger sequencing negative results were predicted by age, tumor size, and systolic blood pressure values. However, these variables were no longer useful for the prediction when the VAF was entered in a refined regression analysis in the smaller cohort of 48 patients with uPA submitted to both Sanger and NGS sequencing. Accordingly, a low VAF was identified as the major and only determinant of Sanger sequencing negative results.

Thus, these findings evidenced that: (i) Sanger sequencing does not permit the detection of KCNJ5 mutations in a substantial proportion of the cases when the rate of mutated aldosterone-producing cells is low; and (ii) NGS identified

Table 4. Mutation identified by NGS in KCNJ5-positive PA patients at Sanger

Patient number	*KCNJ5* mutation	VAF (%)	Gene_2	c.DNA	Amino acid change	VAF (%)
2	p.Leu168Arg	27.1	*CTNNB1*	c.133T > C	p.Ser45Pro	27.15
15	p.Gly151Arg	18.8	*CTNNB1*	c.133T > C	p.Ser45Pro	26.3
168	p.Gly151Arg	31	*CACNA1H*	c.6013C > T	p.Arg2005Cys	47
82	p.Gly151Arg	37.5	*ATP2B3*	c.1272_1277del	p.Lys402_Phe404delinsAsn	37.3
83	p.Leu168Arg	28.4	*CLCN2*	dupCGG	p.Arg646-Gln647insArg	36.9
162	p.Leu168Arg	34.1	*CACNA1H*	c.6013C > T	p.Arg2005Cys	47.8
137	p.Gly151Arg	32.5	*CLCN2*	c.1795G > A	p.Asp599Asn	49.5
138	p.Leu168Arg	17	*GNAq*	c.286A > T	p.Thr96Ser	8
87	p.Leu168Arg	15	*ATP2B3*	c.1230_1235delGCTGGT	p.Leu411del	10
103	p.Gly151Arg	31.2	*CTNNB1*	c.133T > C	p.Ser45Pro	12.8
114	p.Leu168Arg	31.8	*CLCN2*	dupCGG	p.Arg646-Gln647insArg	44
171	p.Gly151Arg	35.8	*CLCN2*	dupCGG	p.Arg646-Gln647insArg	43.4

Abbreviations: *ATP2B3*, ATPase Ca^{2+}-transporting, plasma membrane 3; *CACNA1H*, Calcium channel, voltage-dependent, T-type, 1H-subunit; *CLCN2*, Chloride Voltage-Gated Channel 2; *CTNNB1*, β-catenin; *GNAq*, Guanine Nucleotide Binding Protein (G Protein); VAF, variant allele frequency.

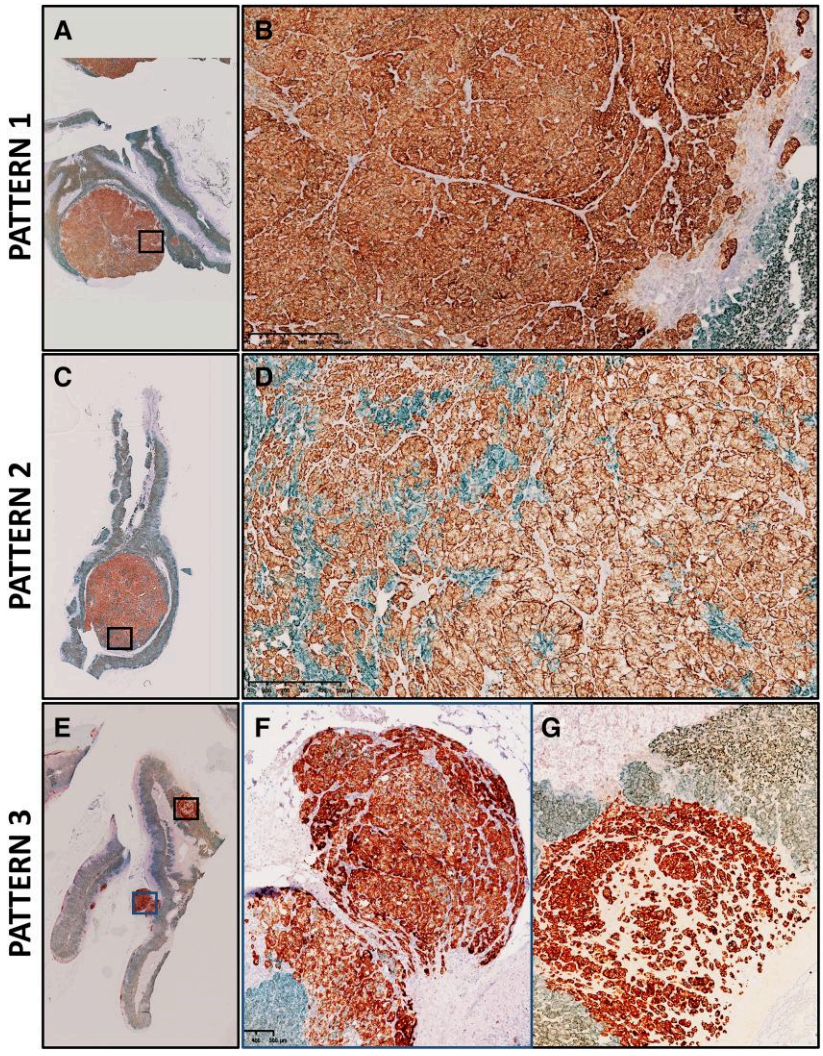

Figure 3. Representative double CYP11B1/CYP11B2 immunohistochemical staining of resected adrenal glands of patients with uPA. Panels A and B demonstrate pattern 1: the adenoma is homogeneously immunolabelled for CYP11B2 (in brown) with only scant cells expressing CYP11B1 (in green). Panels C and D illustrate pattern 2: the adenoma is immunolabelled for both CYP11B2 and CYP11B1. Panels E shows an example of pattern 3: in the adrenal gland there are multiple nodules positive for CYP11B2 shown at higher magnification in panels F and G. Images were carried out using a DM 2000 (Leica, Wetzlar, Germany) microscope.

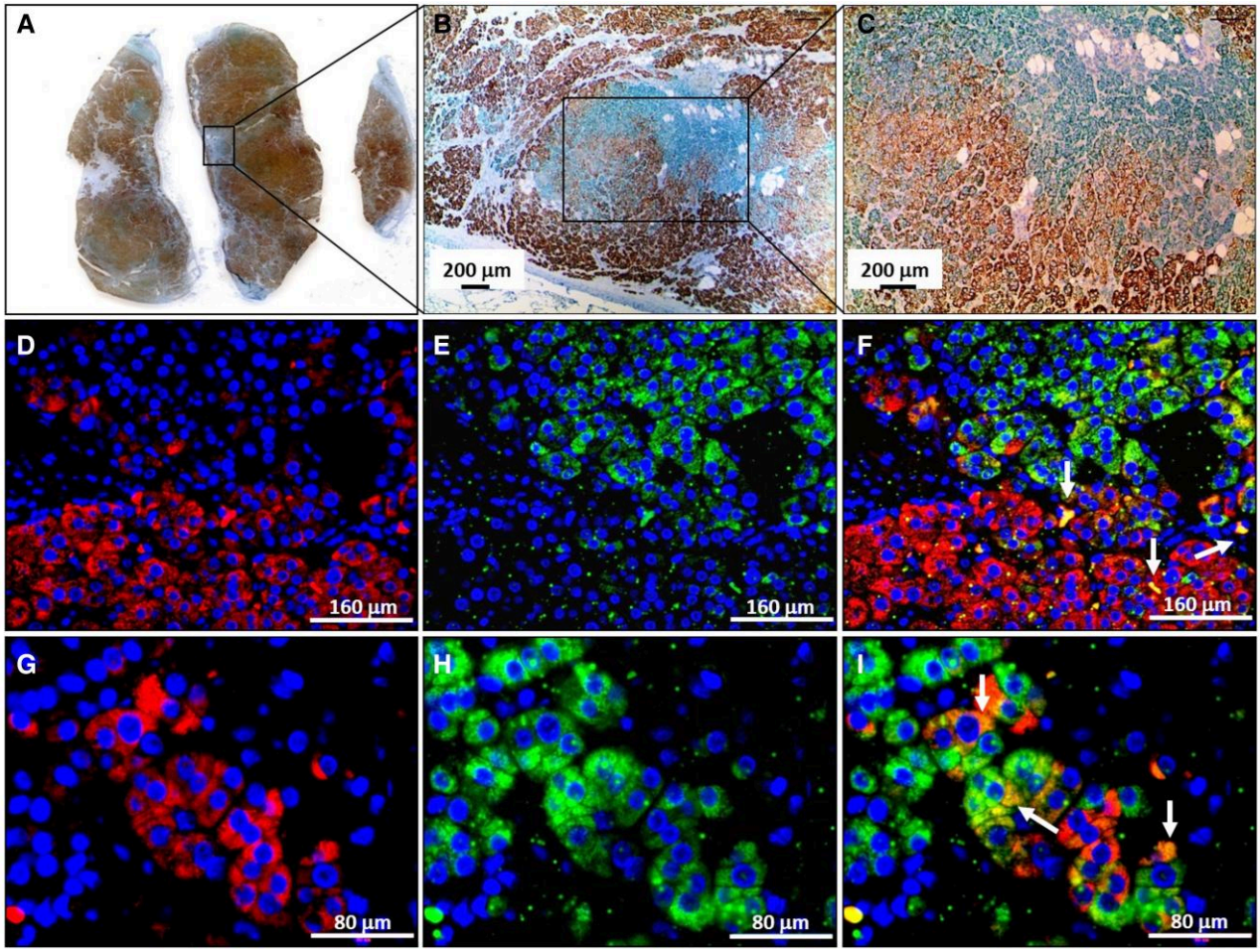

Figure 4. Panels A, B, and C show CYP11B2/CYP11B1 immunohistochemical staining at different magnification in an IHC pattern 2 KCNJ5-mutated APA. The adenoma is immunostained with monoclonal antibodies for both CYP11B2 (in brown) and CYP11B1 (in green). Panels from D to I show confocal analysis of double CYP11B2 (in red)/CYP11B1 (in green) immunofluorescence in the same APA. They clearly show that the tumor comprised 3 different cell populations: one expressing only CYP11B2, one expressing only CYP11B1 cells, and one, made of much fewer cells (identified in orange in the merged panel F and I), that co-express both enzymes, as indicated by the arrows. For immunofluorescence images the slides were photographed using an Eclipse Nikon Microscope with a Rover camera and pseudocolored.

Table 5. KCNJ5 mutations at Sanger sequencing and their distribution among the different patterns identified with immunohistochemistry

IHC * KCNJ5 Sanger Sequencing Crosstabulation

			Sanger KCNJ5 Sequencing		Total
			Mutated	Wild-type	
IHC	Pattern 1	Count	10	21	31
		Expected Count	13.7	17.3	31.0
	Pattern 2	Count	40	21	61
		Expected Count	26.9	34.1	61.0
	Pattern 3	Count	6	29	35
		Expected Count	15.4	19.6	35.0
Total		Count	56	71	127
		Expected Count	56.0	71.0	127.0

Chi-Square Tests

	Value	df	Asymptotic Significance (2-sided)
Pearson Chi-Square	22.492[a]	2	<.001
Likelihood Ratio	24.682	2	<.001
Linear-by-Linear Association	2.030	1	.154
N of Valid Cases	127		

[a]Indicates 0 cells (.0%) have expected count less than 5. The minimum expected count is 13.67.

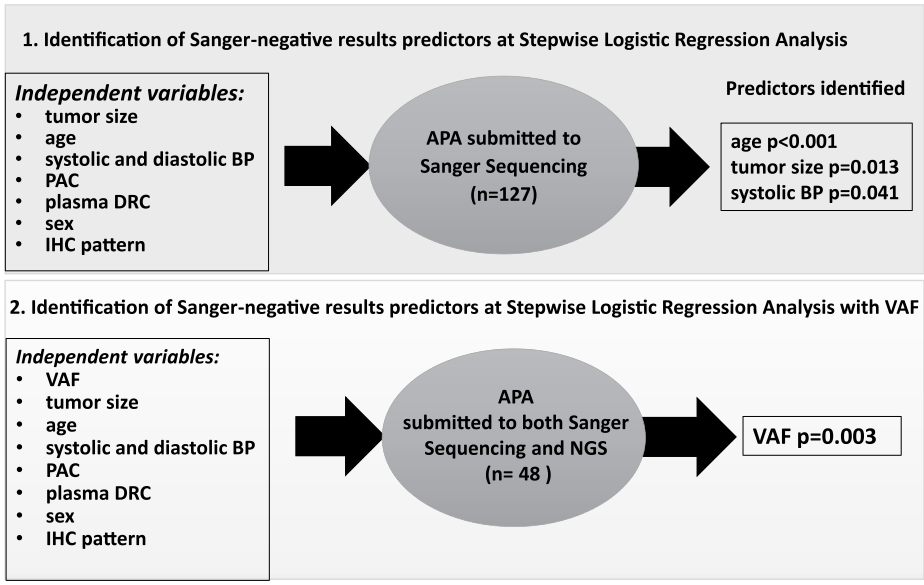

Figure 5. Representation of the 2 stepwise (back) regression models that were used to identify the determinants of Sanger-negative KCNJ5 somatic mutations. The first model was applied to the entire cohort, while the second to a smaller cohort submitted to both Sanger and NGS, because only the latter method furnishes the VAF. Please note how, despite the much smaller sample size, the VAF emerged as the strongest predictor and rendered the other predictors useless to the model.

these false negative cases, because it provided the sensitivity that is needed to analyze heterogeneous tissues as APA tumors, where only few cells can carry the mutations.

The IHC guidance of sequencing was used to enhance the percentage of aldosterone-producing cells in the adrenal specimen and, therefore, to increase the sensitivity for the detection of KCNJ5 mutations (9, 10). To investigate how the performance of the NGS method used in this study compared to available data, we examined the *KCNJ5* mutation rate reported in studies where the APA negative at Sanger sequencing were retested with a protocol entailing IHC-guided NGS (9, 10).

We found that the prevalence rate of KCNJ5 mutations found with NGS and Sanger in our study was 6% higher than found by De Sousa et al (44%) (10), and 12% higher than reported by Hacini et al (38%) (9). To date, a higher 73% rate of *KCNJ5* mutations was reported in only one study carried out in Japan by Nanba et al (5); however, this could be partially due to the much higher prevalence (63%) of somatic mutations in *KCNJ5* in East Asian countries that was documented in a large meta-analysis of studies from different continents, as the authors acknowledged (14).

As regarding IHC-guided sequencing, by systematically using double IHC for CYP11B2 and CYP11B1, we found that 74% of KCNJ5-mutated APA belonged to pattern 2, whereas CYP11B2 expressing APA (pattern 1) carried a much lower rate (12%) of KCNJ5 mutations, similar to the rate seen in pattern 3 (Fig. 3). Moreover, confocal microscopy analysis of a pattern 2 APA submitted to double immunofluorescence studies highlighted the existence of 3 cell populations and showed that a small subset of cells co-expressed CYP11B2 and CYP11B1 (Fig. 4). Thus, results obtained by selecting only CYP11B2-positive cells or areas, as done in IHC-guided sequencing studies (9, 10), could not be representative of the mutational status of the entire specimen. Moreover, these results raise the question on whether CYP11B1-positive or CYP11B1/CYP11B2 cells in IHC pattern 2 contribute to the KCNJ5 mutation, an issue that mandates further specific research.

The NGS technology reduces the time from sampling to reporting and has allowed a broader application of molecular profiling in human tumors (5). Compared to Sanger, NGS sequencing has, besides a higher sensitivity, the advantage of allowing detection of mutations occurring in multiple spots of one or more genes, which is crucial when searching for somatic variants in resected adrenals of PA patients that often carry more than one mutation in multiple genes and in different areas and nodules (29). In line with this, in our specimens that were either Sanger-negative or NGS-positive for KCNJ5 mutations, NGS unveiled additional variants in other genes (Table 3).

There are limitations and strengths to be acknowledged in this study: the first is that a head-to-head comparison of IHC-guided and non-IHC-guided Sanger, or NGS sequencing in the same patients could not be performed. Therefore, even though the available data support the contention that non-IHC-guided NGS has a similar sensitivity as IHC-guided sequencing for the detection of *KCNJ5* mutations (9, 10), the lack of direct comparison suggests caution in concluding that unguided NGS is better than, or equivalent to, IHC-guided targeted sequencing. This limitation is counterweighed by several strengths, including a rather large cohort of consecutive patients conclusively diagnosed as having uPA at biochemical retesting after surgery, alongside the systematic use of double CYP11B2 and CYP11B1 IHC with specific human monoclonal antibodies, and of a high resolution state-of-the-art NGS.

In summary, these results showed that double CYP11B2 and CYP11B1 immunostaining affects the rate of KCNJ5 mutations and that NGS has a sensitivity higher than Sanger and probably not lower than that reported with IHC-guided approaches (9, 10). These findings can contribute to expand the application of molecular profiling of resected adrenals to centers that cannot apply the time-consuming and technically demanding protocols that require IHC for selection of the

tumor areas, thus representing a major step toward exploiting precision medicine strategies for the management of patients with PA carrying KCNJ5 mutations, whose detection can lead to targeted pharmacological treatment with macrolide antibiotics and their derivatives (15-17).

Funding

This study was supported by the following research grants: FORICA (The Foundation for Advanced Research in Hypertension and Cardiovascular Diseases) to G.P.R.; CORIS-Consorzio per la Ricerca Sanitaria (project code ROSS_PRIV20_04); University of Padua DOR to G.P.R. and B.C.; and DIMAR Excellence project funding (DImed and Rare Diseases) of the Department of Medicine, by the University of Padua.

Disclosures

The authors have nothing to disclose.

Data Availability

Data generated during the current study are not publicly available but are available from the corresponding author on reasonable request.

References

1. Choi M, Scholl UI, Yue P, *et al.* K+ channel mutations in adrenal aldosterone-producing adenomas and hereditary hypertension. *Science*. 2011;331(6018):768-772.
2. Seccia TM, Caroccia B, Gomez-Sanchez EP, Gomez-Sanchez CE, Rossi GP. The biology of normal zona Glomerulosa and aldosterone-producing adenoma: pathological implications. *Endocr Rev*. 2018;39(6):1029-1056.
3. Boulkroun S, Beuschlein F, Rossi G-P, *et al.* Prevalence, clinical, and molecular correlates of KCNJ5 mutations in primary aldosteronism. *Hypertension*. 2012;59(3):592-598.
4. Lenzini L, Rossitto G, Maiolino G, Letizia C, Funder J, Rossi GP. A meta-analysis of somatic KCNJ5 K+ channel mutations in 1636 patients with an aldosterone-producing adenoma. *J Clin Endocrinol Metab*. 2015;100:E1089-E1095.
5. Nanba K, Omata K, Else T, *et al.* Targeted molecular characterization of aldosterone-producing adenomas in white Americans. *J Clin Endocrinol Metab*. 2018;103(10):3869-3876.
6. Salk JJ, Schmitt MW, Loeb LA. Enhancing the accuracy of next-generation sequencing for detecting rare and subclonal mutations. *Nat Rev Genet*. 2018;19(5):269-285.
7. Nakamura Y, Maekawa T, Felizola Saulo JA, Satoh FQX. Adrenal CYP11B1/2 expression in primary aldosteronism: immunohistochemical analysis using novel monoclonal antibodies. *Physiol Behav*. 2014;176(1):139-148.
8. Nanba K, Yamazaki Y, Bick N, *et al.* Prevalence of somatic mutations in aldosterone-producing adenomas in Japanese patients. *J Clin Endocrinol Metab*. 2020;105(11):1-8.
9. Hacini I, de Sousa K, Boulkroun S, *et al.* Somatic mutations in adrenals from patients with primary aldosteronism not cured after adrenalectomy suggest common pathogenic mechanisms between unilateral and bilateral disease. *Eur J Endocrinol*. 2021;185(3):405-412.
10. De Sousa K, Boulkroun S, Baron S, *et al.* Genetic, cellular, and molecular heterogeneity in adrenals with aldosterone-producing adenoma. *Hypertension*. 2020;75(4):1034-1044.
11. Azizan EA, Poulsen H, Tuluc P, *et al.* Somatic mutations in ATP1A1 and CACNA1D underlie a common subtype of adrenal hypertension. *Nat Genet*. 2013;45(9):1055-1060.
12. Beuschlein F, Boulkroun S, Osswald A, *et al.* Somatic mutations in ATP1A1 and ATP2B3 lead to aldosterone-producing adenomas and secondary hypertension. *Nat Genet*. 2013;45(4):440-4.444e1-2.
13. Scholl UI, Goh G, Stolting G, *et al.* Somatic and germline CACNA1D calcium channel mutations in aldosterone-producing adenomas and primary aldosteronism. *Nat Genet*. 2013;45(9):1050-1054.
14. Itcho K, Oki K, Ohno H, Yoneda M. Update on genetics of primary aldosteronism. *Biomedicines*. 2021;9(4):409.
15. Maiolino G, Ceolotto G, Battistel M, *et al.* Macrolides for KCNJ5–mutated aldosterone-producing adenoma (MAPA): design of a study for personalized diagnosis of primary aldosteronism. *Blood Press*. 2018;27(4):200-205.
16. Caroccia B, Prisco S, Seccia TM, Piazza M, Maiolino G, Rossi GP. Macrolides blunt aldosterone BiosynthesisNovelty and significance. *Hypertension*. 2017;70(6):1238-1242.
17. Scholl UI, Abriola L, Zhang C, *et al.* Macrolides selectively inhibit mutant KCNJ5 potassium channels that cause aldosterone-producing adenoma. *J Clin Invest*. 2017;127(7):2739-2750.
18. Gioco F, Seccia TM, Gomez-Sanchez EP, Rossi GP, Gomez-Sanchez CE. Adrenal histopathology in primary aldosteronism: is it time for a change? *Hypertension*. 2015;66(4):724-730.
19. Funder JW, Carey RM, Mantero F, *et al.* The management of primary aldosteronism: case detection, diagnosis, and treatment: an endocrine society clinical practice guideline. *J Clin Endocrinol Metab*. 2016;101(5):1889-1916.
20. Rossi GP, Bisogni V, Bacca AV, *et al.* The 2020 Italian society of arterial hypertension (SIIA) practical guidelines for the management of primary aldosteronism. *Int J Cardiol Hypertens*. 2020;5:100029.
21. Rossi GP. Primary aldosteronism: jACC state-of-the-art review. *J Am Coll Cardiol*. 2019;74(22):2799-2811.
22. Rossi GP, Ceolotto G, Rossitto G, *et al.* Prospective validation of an automated chemiluminescence-based assay of renin and aldosterone for the work-up of arterial hypertension. *Clin Chem Lab Med*. 2016;54(9):1441-1450.
23. Kuppusamy M, Caroccia B, Stindl J, *et al.* A novel KCNJ5-insT149 somatic mutation close to, but outside, the selectivity filter causes resistant hypertension by loss of selectivity for potassium. *J Clin Endocrinol Metab*. 2014;99(9):E1765-E1773.
24. Williams TA, Lenders JWM, Mulatero P, *et al.* Outcomes after adrenalectomy for unilateral primary aldosteronism: an international consensus on outcome measures and analysis of remission rates in an international cohort. *Lancet Diabetes Endocrinol*. 2017;5(9):689-699.
25. Uhlen M, Quake SR. Sequential sequencing by synthesis and the next-generation sequencing revolution. *Trends Biotechnol*. 2023;41(12):1565-1572.
26. Menard S. *Applied logistic regression analysis. Series on quantitative applications in the social sciences*. Sage University Papers; 2001.
27. Caroccia B, Lenzini L, Ceolotto G, *et al.* Supplemental Material "Double CYP11B1/CYP11B2 Immunohistochemistry and Detection of KCNJ5 Mutations in Primary Aldosteronism". Research Data Unipd. 2024. https://researchdata.cab.unipd.it/id/eprint/1218. Deposited 5 March 2024.
28. Nanba K, Omata K, Gomez-Sanchez CE, *et al.* Genetic characteristics of aldosterone-producing adenomas in blacks. *Hypertension*. 2019;73(4):885-892.
29. Scholl UI. Genetics of primary aldosteronism. *Hypertension*. 2022;79(5):887-897.